Original Research Report

IMPACT ON THE KIDNEY OF PANCREAS DAMAGE DUE TO STREPTOZOTOCIN-INDUCED HYPERGLYCEMIA

Yana Aurora Prathita[1,2*], Ahmad Aulia Jusuf[3], Christina Simadibrata[4], Wahyuningsih Djaali[5,6], Yoshua Viventius[5,7]

[1]Master's Program in Biomedical Sciences, Faculty of Medicine, Universitas Indonesia, Jakarta, Indonesia
[2]Faculty of Medicine, Universitas Sultan Ageng Tirtayasa, Serang, Banten, Indonesia
[3]Department of Histology, Faculty of Medicine, Universitas Indonesia, Jakarta, Indonesia
[4]Department of Medical Acupuncture, Faculty of Medicine, Universitas Indonesia, Jakarta, Indonesia
[5]Medical Acupuncture Specialist Program, Faculty of Medicine, Universitas Indonesia, Jakarta, Indonesia
[6]Universitas Negeri Jakarta, Jakarta, Indonesia
[7]Dr. Cipto Mangunkusumo National Central Public Hospital, Jakarta, Indonesia

ABSTRACT

The kidneys are one of the organs affected by microvascular complications due to diabetes mellitus. Hyperglycemia plays an important role in glomerular, mesangial cell, and tubular damage in the kidneys. Metabolic dysregulation, including hyperglycemia, initiates cellular damage in the kidneys. Streptozotocin (STZ) is a chemical compound that is known to damage pancreatic cells and cause hyperglycemia. This study aimed to examine the effects of hyperglycemia on the morphology of the kidneys. Kidney tissues were observed histologically using a light microscope. Samples were taken from the kidneys of experimental animals administered with STZ to induce hyperglycemia. Observation was performed afterwards to investigate any damage to pancreatic cells. A total of 12 kidney samples were divided into two groups: the control group and the STZ-induced group. The samples were prepared before staining with hematoxylin-eosin and Masson's trichrome. The endothelium, podocytes, mesangial cells, and basement membrane of the glomerulus were examined. The tubules of the kidneys were also examined, and the presence or absence of connective tissue formation in both groups was statistically tested. The results suggested a significant difference in tubular damage ($p<0.05$) and an insignificant difference in an increase in the damage of other components of the kidneys ($p>0.05$) in the STZ-induced group. Significant morphological changes were observed in the hyperglycemic renal tubules due to the administration of STZ. In conclusion, STZ-induced hyperglycemia caused damage to the kidney components but overall had no significant impact on the kidney.

Keywords: Diabetes mellitus; glomerulus; streptozotocin (STZ); tubular damage

***Correspondence:** Yana Aurora Prathita, Master's Program in Biomedical Sciences, Faculty of Medicine, Universitas Indonesia, Jakarta; Faculty of Medicine, Universitas Sultan Ageng Tirtayasa, Serang, Banten, Indonesia. Email: yanaauroraprathita@gmail.com

Article history
●Submitted 13/2/2023 ● Revised 4/5/2023 ● Accepted 26/5/2023 ● Published 10/6/2023

How to cite: Prathita YA, Jusuf AA, Simadibrata C, et al (2023). Impact on the Kidney of Pancreas Damage due to Streptozotocin-Induced Hyperglycemia. Folia Medica Indonesiana, 59 (2), 156-163, https://doi.org/10.20473/fmi.v59i2.33584

pISSN: 2355-8393, eISSN: 2599-056x

Highlights:
1. This study observed the histology of pancreatic β-cell damage without any intervention to the kidneys of the animal models.
2. The histological analysis of the kidneys shows that STZ-induced animal models can be used for assessing kidney abnormalities due to hyperglycemia.
3. A scoring system for the histological analysis was developed to evaluate the changes in the kidney cells.

INTRODUCTION

Streptozotocin (STZ) is a glucose molecule derived from the *Streptomyces griseus* soil bacterium. The bacteria can be used for a broad-spectrum antibiotic that is toxic to pancreatic β-cells (Sundaram et al. 2019). STZ has been shown to selectively harm pancreatic islet cells, resulting in hyperglycemia. The chemical compounds in STZ can be used to investigate tissue damage caused by diabetes. This is important for developing experimental animal models, such as rats, mice, and monkeys. In recent

years, STZ has become the drug of choice for inducing diabetes, especially in rodents, due to its complications (Furman 2015, Giralt-López et al. 2020). The administration of STZ in 50–65 mg/kg doses can cause hyperglycemia without severe ketosis.

The degenerative nature of diabetes mellitus complications results in high mortality and morbidity rates. The World Health Organization reported an increase in the prevalence of type 2 diabetes mellitus globally. Furthermore, the International Diabetes Federation reported that there was an increase in the number of people with type 2 diabetes mellitus between 2013 and 2017. By the year 2045, it was estimated that the number would increase to 693 million (Cho et al. 2018). In the 2018 Basic Health Research report by the Indonesian Ministry of Health, there was an increase of 8.5% in the prevalence of type 2 diabetes mellitus. As the prevalence of diabetes mellitus increased, the probability of complications, such as microvascular, macrovascular, and nervous system disorders, also increased (Soelistijo et al. 2021).

One of the organs affected by microvascular complications caused by diabetes is the kidney. Chronic kidney disease is a potential impact of diabetes mellitus. Moreover, diabetes is the single most common cause of end-stage chronic kidney disease. Approximately 20–40% of diabetes mellitus patients will develop diabetic nephropathy, which is the cause of end-stage chronic kidney disease (Ameh et al. 2019). Hyperglycemia is an important factor in the development of glomerular, mesangial, and tubular damage in the kidney. Kidney cellular damage is initiated by metabolic dysregulation, including hyperglycemia, hyperlipidemia, and insulin resistance. Increased reactive oxygen species due to mitochondrial dysfunction in diabetes is a primary event in the development of complications (Reidy et al. 2014). The role of mesangial cells is to maintain the structure of the glomerular capillaries and regulate glomerular filtration through smooth muscle activity. Hyperglycemia boosts the proliferation and hypertrophy of mesangial cells through increased reactive oxygen species in the cells. This can lead to an increase in matrix production as well as thickening of the basement membrane. Hyperglycemia can also cause an increased expression of vascular endothelial growth factor, which results in increased vascular permeability (Khan et al. 2020). Damage to the glomerulus due to prolonged hyperglycemia can lead to decreased kidney function. Large molecules, such as protein and glucose, can pass through the filtration process if the function of glomerular filtration is compromised. In addition, the function of fluid reabsorption in the renal tubules is also impaired if hyperglycemia occurs.

Long-term hyperglycemia can induce hypoxia, resulting in scar tissue as a response. Fibroblasts in the renal interstitium will differentiate into fibrocytes and fill most of the kidney tissue. Hyperglycemia, in conjunction with transforming growth factor beta (TGF-β), angiotensin (AngII), and advanced glycation end products (AGEs), will induce epithelial-mesenchymal transition (EMT). Additionally, it increases alpha smooth muscle actin (α-SMA) and vimentin expressions, downregulates E-cadherin, damages the epithelial layer, and alters the phenotype of mesenchymal cells, resulting in the formation of scar tissue (Braga et al. 2022). These conditions will clearly worsen kidney function. In the late stages, the renal interstitial space will be filled with scar tissue. A recent study showed that intermittent or chronic hyperglycemia plays an important role in the initiation and persistence of diabetes mellitus complications, including kidney disease (Amorim et al. 2019). This study aimed to determine whether pancreatic beta cell damage that causes hyperglycemia has a direct impact on the kidney. A histological assessment was conducted to observe the presence of the impact.

MATERIALS AND METHODS

This study was part of a larger study by Jusuf et al. (2021) on the effectiveness of manual acupuncture at the EX-B3 Weiwanxianshu point. The study observed the histological images of the pancreas and blood sugar levels of rats with type 2 diabetes. In accordance with the ethical guidelines for the use of animal models in medical research, this study used kidney samples collected from experimental male Sprague-Dawley rats aged 8–10 weeks. The rats were divided into two groups of six, consisting of the control group and the STZ-induced group. The rats in the STZ-induced group received 50 mg of STZ. The dose was expected to be sufficient to cause pancreatic cell damage (Goyal et al. 2016).

The kidneys were fixed in 10% formol saline and then dehydrated using graded alcohol at 70%, 80%, 95%, and 100% (2x). After being cleansed with xylol, the kidneys appeared clear. The next stage was embedding the organs in liquid paraffin or Paraplast at a temperature of ±60°C. Following the procedure was the casting (blocking) process using plastic molds and metal plates. The plastic mold was placed on a metal plate. A small amount of liquid Paraplast was poured into the molds, and then the organs were inserted and positioned in the Paraplast. The liquid Paraplast was then poured again until it covered the entire mold. Paraffin blocks that had been made were left to harden before further

processing. The tissue of the kidneys was then cut using a microtome with a thickness of 5 mm. The samples were then stained with hematoxylin-eosin (HE) and Masson's trichrome (Mondal 2017).

Renal histology was observed, particularly on the glomerulus and renal tubules (proximal and distal convoluted tubules in the cortex). Hematoxylin and eosin staining and Masson's trichrome staining were used to observe any increase in collagen (fibrosis). The observation was performed using 4x10 magnification with five fields of view, i.e., top left, bottom left, top right, bottom right, and middle. There would be 10x magnification in each field of view. Glomerulus and renal tubules would be observed with a magnification of 40x10 (Rezk et al. 2017).

The observed parts of the glomerulus included capillaries, podocytes, and mesangial tissue. Capillary observation was focused on endothelial cell damage. The degree of capillary endothelial cell damage was calculated in each field of view of the glomerulus. The calculation was carried out by determining the percentage of capillary endothelial cell damage, as indicated by pyknotic nuclei or the detachment of cells from the basement membrane (Mondal 2017). The calculation was performed using the following formula.

$$\frac{\Sigma \text{ damaged endothelial cells}}{\Sigma \text{ total endothelial cell}} \; x \; 100\%$$

The average percentage of capillary damage in one field of view was calculated by dividing the number of damaged capillaries in each glomerulus by the number of glomeruli and multiplied by 100% (Levey et al. 2014).

$$\frac{\Sigma \text{ percentage of glomerular capillary damage in each glomerulus}}{\Sigma \text{ glomerulus in 5 fields of view}} \; x100\%$$

Observation of podocytes was focused on the presence or absence of visceral thickening of Bowman's capsule and podocyte cell damage in the visceral Bowman's capsule. The visceral thickening of Bowman's capsule was determined by comparing the thickness of the membrane of Bowman's capsule to that of podocyte cells. Podocyte damage was characterized by pyknotic nuclei or cells detached from the basement membrane (Nagata 2016, Kopp et al. 2020).

The level of podocyte cell damage in each field of view of the glomerulus was calculated by determining the percentage of podocyte cell damage with the formula formula (Levey et al. 2014).

$$\frac{\Sigma \text{ damaged podocytes}}{\Sigma \text{ total podocytes}} \; x \; 100\%$$

The average podocyte cell damage in one field of view was calculated by dividing the percentage of podocyte cell damage in each glomerulus by the number of glomeruli and then multiplying the result by 100% (Levey et al. 2014).

$$\frac{\Sigma \text{ percentage of podocyte cell damage in each glomerulus}}{\Sigma \text{ glomerulus in 5 fields of view}} \; x100$$

The degree of damage to Bowman's capsule pars visceral was calculated by comparing the size of the podocyte with the basement membrane. If the podocyte was larger than the mass membrane, it would indicate that there was no thickening of the basement membrane (Inker et al. 2016). The degree of the damage was calculated by dividing the number of thickened Bowman's capsules in one field of view by the number of glomeruli observed, as seen in the formula below.

$$\frac{\Sigma \text{ thickening of Bowman's capsule pars visceral}}{\Sigma \text{ glomerulus observed in 5 fields of view}} \; x \; 100\%$$

In the observation of mesangial tissue, the tissue inflammation was characterized by inflammatory cell powder and mesangial cell density. The maximum damage in one field of view was recorded. In the mesangial network scoring system, A score of 0 would indicate the presence of <10 inflammatory cells. A score of 1 would indicate that 10–20 inflammatory cells were present. A score of 2 would indicate twenty to thirty inflammatory cells. Moreover, a score of 3 would indicate the presence of >30 inflammatory cells (Inker et al. 2016). The density of mesangial cells was calculated using the following formula.

$$\frac{\Sigma \text{ mesangial cells}}{\text{glomerular area}}$$

Damage to the proximal and distal convoluted tubules of the kidney is defined as tubular atrophy. This condition would be characterized by either pyknotic nuclei, vacuolization of the cytoplasm, shedding of epithelial cells, or thickening of the tubular basement membrane (Pourghasem et al. 2015). The average number of injuries observed in each field of view was then calculated. The percentage of tubular injuries was calculated using the following formula.

$$\frac{\Sigma \text{ tubule damaged}}{\Sigma \text{ total tubule in one field of view}} \; x100\%$$

Observation of fibrosis was performed in the renal cortex using Masson's trichrome staining. Descriptive observations were conducted on the glomerulus and renal tubules. Statistical analysis was performed using IBM SPSS Statistics for Windows, version 25.0 (IBM Corp., Armonk, N.Y., USA). The data were tested for normality and

homogeneity using the Saphiro-Wilk test and the Levene test. Comparison between groups of each parameter was tested by the Chi-square test ($p<0.05$). If there was a significant difference between groups, it would be followed by the least significant difference (LSD) multiple comparison test (Furman 2015).

RESULTS

The percentage of morphological changes in endothelial cells and podocyte cells in the STZ-induced group increased compared to the control group. The number of morphological changes in the control group of endothelial cells was 3.11±3.90%, while in the STZ-induced group it was 6.01±5.35%. Podocyte cells in the control group underwent morphological changes of 2.96±3.32%, while the STZ-induced group experienced morphological changes of 6.17±2.32% (Table 1). The percentage of damage to each kidney component in the control group and the STZ-induced group did not differ significantly for the endothelium and podocytes ($p>0.05$). However, significant differences were shown in the tubules ($p<0.05$), as shown in Figure 1. The mesangial density was 0.0076±0.0013 in the control group and 0.0061±0.0008 in the STZ-induced group. A statistical test between the groups showed no significant difference ($p>0.05$), as shown in Figure 2.

Table 1. Value of damage to kidney components according to the test results.

Parameters	Control group	STZ-induced group
Endothelial cells (%)	3.11±3.90	6.01±5.35
Podocytes (%)	2.96±3.32	6.17±2.32
Tubules (%)	5.06±1.97	9.44±1.64*
Mesangial density (mean)	0.0076± 0.0013	0.0061±0.0008

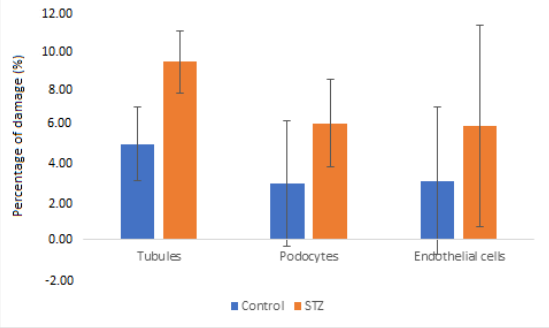

Figure 1. The percentage of damage to each kidney component in the control group and the STZ-induced group.

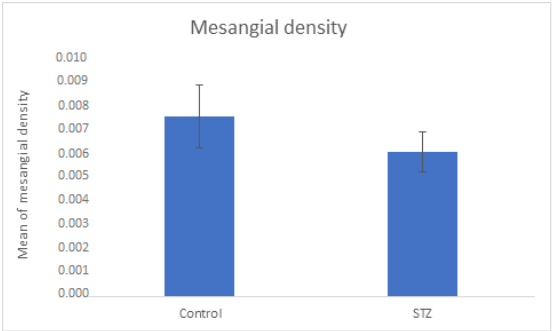

Figure 2. The mean of mesangial density in the control group and the STZ group.

Figure 3a shows the morphological changes of podocytes with pyknotic nuclei. The percentage of the changes increased, but there was no statistically significant difference ($p>0.05$). No inflammatory cells were found in the interstitial glomerulus in the control group or the STZ-induced group. In observing the thickening of the basement membrane, the membrane thickness was compared to the podocyte width. No basement membrane thickening was found.

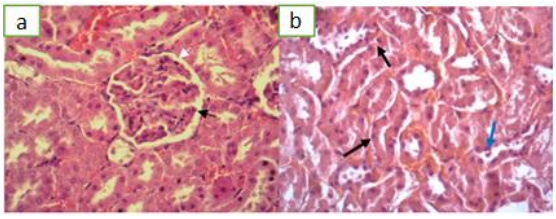

Figure 3. Hematoxylin-eosin staining of the STZ-induced group with 40x10 magnification: (a) In the glomerulus, pyknotic nuclei (black arrows) were seen in visceral podocytes, and normal nuclei (white arrows) were seen in the podocytes; (b) In the tubules, pyknotic nuclei (black arrows) were seen in tubular cells, and cells detached from the basement membrane (blue arrows).

Tubular examination using hematoxylin-eosin staining on the renal cortex showed an increase in the percentage of tubular cells with pyknotic nuclei of 9.44±1.64% in the STZ-induced group compared to 5.06±1.97% in the control group. A statistical test showed that there were significant differences between the two groups, with $p<0.05$. Microscopic observation of the proximal and distal convoluted tubules under 40x10 magnification revealed a significant difference in the STZ-induced group compared to the control group, with a p-value of 0.05. Pyknotic nuclei in the cells and separation of cells from the basement membrane indicated morphological changes in each group (Figure 3b).

The STZ-induced group displayed the most significant morphological changes.

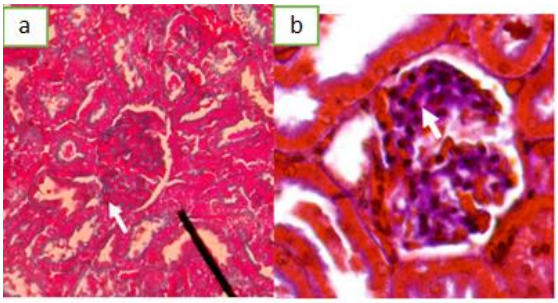

Figure 4. Masson's trichrome smear with 40x10 magnification: (a) In the control group, the glomerulus appeared blue only on the basement membrane; (b) In the STZ-induced group, it appeared in a faint blue color on the interstitial glomerulus (white arrows).

The glomerulus, tubules, and interstitial images appeared normal in the control group. The blue stain of collagen fibers was only found in the basement membrane. Glomerulus in the STZ-induced group showed a more diffuse blue stain than in the control group. Kidney samples from the control group showed blue staining in the renal capsule, tubular basement membrane, and glomerular capillary basement membrane (Figure 4a). In the STZ-induced group, blue-stained fibers were observed not only in the basement membrane of the glomerular capillaries but also in the glomerular mesangial tissue, although less clearly (Figure 4b).

DISCUSSION

This study examined the histological description of various kidney components, including podocytes, endothelium, basement membrane in the glomerulus, and tubules in the renal cortex. Uncontrolled hyperglycemia can lead to dysfunction in these components. It interferes with the permeability of the glomerular membrane, causing kidney damage over time (Anders et al. 2018).

The Animal Models of Diabetes Complications Consortium (AMDCC) of the United States of America (USA) recommends the use of standard animal models for developing renal complications of diabetes by induction of STZ. The recommended STZ administration is a low dose of 50 mg/kg for five consecutive days (Bayrasheva et al. 2016). According to the AMDCC, the use of STZ doses above 50 mg/kg can cause kidney damage not because of the effects of hyperglycemia but because of the direct effect of the STZ. Therefore, the 50 mg/kg dose in this study was expected to have an effect on the kidneys due to hyperglycemia and not because of pancreatic damage due to STZ toxicity.

Glomerular capillaries are a type of fenestrated capillary that allows water to pass rapidly through the capillaries. Capillaries consist of endothelium with flattened nuclei and are more heterochromatic (Mondal 2017). In this study, histological observations of endothelial damage at 40x10 magnification showed that the STZ-induced group had more changes in the morphology of endothelium compared to the control group. However, the statistical analysis showed no significant difference in each group ($p>0.05$). The observations revealed that the capillary endothelium had a flattened nucleus and a more heterochromatic staining pattern. Reactive oxygen species generated by hyperglycemia in the kidneys will increase nitrite oxide (NO) so that capillary damage can occur. This condition is characterized by endothelial dysfunction, which can be observed microscopically as pyknotic nuclei or separation of the basement membrane (Sol et al. 2020). This study determined that the effect of hyperglycemia on endothelial cells in the glomerulus was either the presence of pyknotic nuclei or the release of endothelial cells.

An increase in podocyte morphological changes may occur due to the presence of advanced glycation end products (AGEs). In kidneys with hyperglycemic conditions, AGEs contribute to an increase in reactive oxygen species. In addition, AGEs play an important role in apoptosis and the release of cells from the basement membrane (Reidy et al. 2014). An increase in podocyte damage in the STZ-induced group indicated elevated apoptotic conditions in the kidney. The damage contributed greatly to apoptosis and cell release from the basement membrane. In the control group, visceral pars podocytes were found to have relatively large cells with euchromatic nuclei. This suggests that hyperglycemia indirectly caused podocyte damage in the STZ-induced group, although the difference was not statistically significant (Lin & Susztak 2016).

Glomerular infiltration and basement membrane thickening are histological changes that can be observed in kidney damage due to diabetes. Hyperglycemia in the renal glomerulus can increase the expression of monocyte chemoattractant protein-1 (MCP-1), a chemokine that regulates the migration and infiltration of inflammatory cells such as macrophages (de M. Bandeira et al. 2013). In this study, no inflammatory cell infiltration was found in the glomerulus. According to a study by Goyal et al. (2016), the diabetogenic activity of STZ that can result in kidney injury was optimally administered in doses of 65 mg/kg. DNA damage and the infiltration of inflammatory cells such as

macrophages were possible with these doses. In this study, STZ injections were administered to the experimental animals only once. It was expected that the STZ injections would be sufficient to induce hyperglycemia and pancreatic cell damage. The duration of hyperglycemia may explain why there was no change in the glomerulus, given that the AMDCC recommends STZ administration for five consecutive days.

The method used in this study for determining the thickening of the basement membrane was by comparing the podocyte cells with the basement membrane. If the podocyte membrane was larger than the basement membrane, there would be no thickening of the basement membrane. The basement membranes in each group had the same pattern, and the podocytes were still larger than the basement membrane. In a number of earlier studies, different findings were obtained from observations using electron microscopy. The findings showed that there was thickening of the basement membranes (Kymioni Vasiliki-Maria et al. 2016, Rezk et al. 2017). A study by Sameni et al. (2016) reported that hyperglycemia-induced oxidative stress caused growth factors (such as transforming growth factor and tissue growth factor) to increase the extracellular matrix. As a result, the basement membranes became thicker. On the other hand, the results obtained from this study were limited due to a lack of tools, which made it difficult to objectively measure the thickness of the basement membrane

The renal tubule plays an important role in the progression of kidney disease due to diabetes. This component is frequently observed in studies of kidney damage (Giralt-López et al. 2020). The STZ-induced group in this study had significant morphological changes in the tubules. Observation of the cells in each group revealed the presence of pyknotic nuclei and the separation of cells from the basement membrane. Previous research showed that there were changes in the tubules of diabetic experimental animal models. In the histology of the tubules, there were flat epithelium and mononuclear cell filtration (Katsuda et al. 2015).

The increase in glucose due to STZ induction in the experimental animal model in this study proved that the initial state of diabetes had its first effect on the renal tubules. The glucose-induced activation of RAS will activate vascular endothelial growth factor. Along with reactive oxygen species, it will activate ornithine decarboxylase. Increased ornithine decarboxylase expression is known to cause renal tubular hypertrophy. Additionally, tubular hypertrophy and cell aging are caused by the induction of TGF-β and cyclin-dependent kinases that cause tubulointerstitial injury (Moonen et al. 2018).

Mesangial cell hypertrophy and fibroblast formation are also seen in kidneys that have been exposed to chronic hyperglycemia for a long time. TGF-β and extracellular matrix stimulation can be triggers for mesangial cell hypertrophy and fibroblast formation (Pourghasem et al. 2015). An analysis of mesangial density can be used to assess whether there is hypertrophy in the mesangial cells. The mesangial density is calculated by dividing the number of mesangial cells by the area of the glomerulus. The results of this study showed that there was no significant difference between the groups in terms of mesangial density in the glomerulus.

Masson's trichrome staining can be used to determine the presence or absence of collagen fibers in response to an increase in reactive oxygen species. This is important as it can lead to an increase in the production of extracellular matrix (Mondal 2017). The appearance of blue staining indicates collagen fibers. The glomerular mesangial tissue in the STZ-induced group showed blue-colored fibers. These findings suggest that the formation of excess extracellular matrix in the glomerulus in the STZ-induced group was due to an increased role of reactive oxygen species, which increased the extracellular matrix production via TGF-β (Sutariya et al. 2016).

Strength and limitations

Our study evaluated every component of the kidney that might be affected by increasing blood glucose levels using microscopy. This study used a scoring system that provided a validated outcome measure. However, microscopic examination and subjective assessment became the limitations of this study. Assessment of the histological aspects in this study involved two people, and each of them confirmed their findings. This study may inspire future studies to use improved scoring of the histological assessment to avoid subjectivity.

CONCLUSION

Hyperglycemia as a result of pancreatic β-cell damage in STZ-induced rats showed a significant difference only in the renal tubules. Other kidney components, such as endothelium, podocytes, and mesangial cells, showed an increase in damage but did not show any significant differences.

Acknowledgment

The authors would like to express their gratitude to Universitas Sultan Ageng Tirtayasa, Serang, Indonesia, for granting the funds for this research. The authors would also like to thank Wahyuningsih Djaali and Yoshua Viventius for providing the

specimens for this research.

Conflict of interest

None.

Ethical consideration

This study received ethical clearance from the Faculty of Medicine, Universitas Indonesia-Dr. Cipto Mangunkusumo National Central Public Hospital, Jakarta, Indonesia, with protocol No. 21-08-0850 on 16/08/2021.

Funding disclosure

This research was funded by a grant from Universitas Sultan Ageng Tirtayasa, Serang, Indonesia.

Author contribution

All authors contributed to the data collection, discussion of the content, and writing, reviewing, and editing of the manuscript before submission.

REFERENCES

Ameh OI, Okpechi IG, Agyemang C, et al (2019). Global, regional, and ethnic differences in diabetic nephropathy. In Diabetic Nephropathy, 33–44. Springer International Publishing, Cham. Available at: http://link.springer.com/10.1007/978-3-319-93521-8_3.

Amorim RG, Guedes G da S, Vasconcelos SM de L, et al (2019). Kidney disease in diabetes mellitus: Cross-linking between hyperglycemia, redox imbalance and inflammation. Arquivos Brasileiros de Cardiologia; doi: 10.5935/abc.20190077

Anders H-J, Huber TB, Isermann B, et al (2018). CKD in diabetes: diabetic kidney disease versus nondiabetic kidney disease. Nature Reviews Nephrology 14**,** 361–377. doi: 10.1038/s41581-018-0001-y

Bayrasheva VK, Babenko AY, Dobronravov VA, et al (2016). Uninephrectomized high-fat-fed nicotinamide-streptozotocin-induced diabetic rats: A model for the investigation of diabetic nephropathy in type 2 Diabetes. Journal of Diabetes Research 2016**,** 1–18. doi: 10.1155/2016/8317850

Braga PC, Alves MG, Rodrigues AS, et al (2022). Mitochondrial pathophysiology on chronic kidney disease. Int J Mol Sci International Journal of Molecular Sciences 23**,** 1776. doi: 10.3390/ijms23031776

Cho NH, Shaw JE, Karuranga S, et al (2018). IDF diabetes atlas: Global estimates of diabetes prevalence for 2017 and projections for 2045. Diabetes Research and Clinical Practice 138**,** 271–281. doi: 10.1016/j.diabres.2018.02.023

Furman BL (2015). Streptozotocin-induced diabetic models in mice and rats. Current Protocols in Pharmacology 70. doi: 10.1002/0471141755.ph0547s70

Giralt-López A, Molina-Van den Bosch M, Vergara A, et al (2020). Revisiting experimental models of diabetic nephropathy. International Journal of Molecular Sciences 21**,** 3587. doi: 10.3390/ijms21103587

Goyal SN, Reddy NM, Patil KR, et al (2016). Challenges and issues with streptozotocin-induced diabetes – A clinically relevant animal model to understand the diabetes pathogenesis and evaluate therapeutics. Chemico-Biological Interactions 244**,** 49–63. doi: 10.1016/j.cbi.2015.11.032

Inker LA, Tighiouart H, Coresh J, et al (2016). GFR estimation using β-Trace protein and β2-microglobulin in CKD. American Journal of Kidney Diseases 67**,** 40–48. doi: 10.1053/j.ajkd.2015.07.025

Jusuf AA, Viventius Y, Djaali W (2021). Comparison between the effectiveness of manual acupuncture and laser acupuncture at EX-B3 weiwanxiashu in a rat model of type 2 diabetes. Journal of Acupuncture and Meridian Studies 14**,** 75–81. doi: 10.51507/j.jams.2021.14.2.75

Katsuda Y, Sasase T, Tadaki H, et al (2015). Contribution of hyperglycemia on diabetic complications in obese type 2 diabetic SDT fatty rats: effects of SGLT inhibitor phlorizin. Experimental Animals 64**,** 161–9. doi: 10.1538/expanim.14-0084

Khan NU, Lin J, Liu X, et al (2020). Insights into predicting diabetic nephropathy using urinary biomarkers. Biochimica et Biophysica Acta (BBA) - Proteins and Proteomics 1868**,** 140475. doi: 10.1016/j.bbapap.2020.140475

Kopp JB, Anders H-J, Susztak K, et al (2020). Podocytopathies. Nature Reviews Disease Primers 6**,** 68. doi: 10.1038/s41572-020-0196-7

Kymioni Vasiliki-Maria, Papamitsoy Theodora, Maggana Ioanna, et al (2016). TGF-b and diabetes mellitus. Journal of Pharmacy and Pharmacology 4. doi: 10.17265/2328-2150/2016.01.001

Levey AS, Inker LA, Coresh J (2014). GFR estimation: From physiology to public health. American Journal of Kidney Diseases 63**,** 820–834. doi: 10.1053/j.ajkd.2013.12.006

Lin JS, Susztak K (2016). Podocytes: the weakest link in diabetic kidney disease? Current Diabetes Reports 16**,** 45. doi: 10.1007/s11892-016-0735-5

de M. Bandeira S, da Fonseca L, da S. Guedes G, et al (2013). Oxidative stress as an underlying contributor in the development of chronic complications in diabetes mellitus. International Journal of Molecular Sciences 14**,** 3265–3284. doi: 10.3390/ijms14023265

Mondal SK (2017). Manual of histological

techniques, illustrate. JP Medical Ltd.

Moonen L, D'Haese P, Vervaet B (2018). Epithelial cell cycle behaviour in the injured kidney. International Journal of Molecular Sciences 19**,** 2038. doi: 10.3390/ijms19072038

Nagata M (2016). Podocyte injury and its consequences. Kidney International 89**,** 1221–1230. doi: 10.1016/j.kint.2016.01.012

Pourghasem M, Shafi H, Babazadeh Z (2015). Histological changes of kidney in diabetic nephropathy. Caspian journal of internal medicine 6**,** 120–7. Available at: http://www.pubmedcentral.nih.gov/articlerender.fcgi?artid=PMC4650785

Reidy K, Kang HM, Hostetter T, et al (2014). Molecular mechanisms of diabetic kidney disease. Journal of Clinical Investigation 124**,** 2333–2340. doi: 10.1172/JCI72271

Rezk HM, El-Sherbiny M, Atef H, et al (2017). Effect of spironolactone on diabetic nephropathy in albino rats: ultrastructural and immunohistochemical study. International Journal of Scientific Reports 3**,** 110. doi: 10.18203/issn.2454-2156.IntJSciRep20171997

Sameni HR, Ramhormozi P, Bandegi AR, et al (2016). Effects of ethanol extract of propolis on histopathological changes and anti-oxidant defense of kidney in a rat model for type 1 diabetes mellitus. Journal of Diabetes Investigation 7**,** 506–513. doi: 10.1111/jdi.12459

Soelistijo SA, Suastika K, Lindarto D, et al (2021). Pedoman pengelolaan dan pencegahan diabetes melitus tipe 2 di Indonesia 2021. PB PERKENI. Available at: https://pbperkeni.or.id/wp-content/uploads/2021/11/22-10-21-Website-Pedoman-Pengelolaan-dan-Pencegahan-DMT2-Ebook.pdf.

Sol M, Kamps JAAM, van den Born J, et al (2020). Glomerular endothelial cells as instigators of glomerular sclerotic diseases. Frontiers in Pharmacology 11. doi: 10.33 89/fphar.2020.573557.

Sundaram R, Nandhakumar E, Haseena Banu H (2019). Hesperidin, a citrus flavonoid ameliorates hyperglycemia by regulating key enzymes of carbohydrate metabolism in streptozotocin-induced diabetic rats. Toxicology Mechanisms and Methods 29**,** 644–653. doi: 10.1080/15376516.2019.1646370

Sutariya B, Jhonsa D, Saraf MN (2016). TGF-β: the connecting link between nephropathy and fibrosis. Immunopharmacology and Immunotoxicology l 38**,** 39–49. doi: 10.3109/08923973.2015.1127382